Investigation on the Narrow Line Seyfert 1 Mrk 335 in an intermediate state, with Chandra/HETGS, NuSTAR and NICER

Rozenn Boissay-Malaquin et al.

rozennbm@umbc.edu

UMBC / NASA Goddard, Greenbelt, MD, USA

The Narrow Line Seyfert 1 Mrk 335 has shown to be highly and rapidly variable in X-ray, both in flux and spectral shape, due to changes in the structure of the hot corona responsible for the primary X-ray emission. Its complex X-ray spectrum presents interesting features that need to be investigated in different states. While several studies have already been performed in low-flux states and during flares, we focus here on the intermediate-flux state, where previously detected warm absorbers are expected to be more easily detectable. After spending two years in a historically long low-flux state, the source finally became brighter in June-July 2020. On this occasion, we performed simultaneous observations of Mrk 335 with NuSTAR, NICER, and first the first time, Chandra/HETGS. We present here our preliminary results regarding the use of NuSTAR observations to constrain the continuum, reflection properties and the broadened Fe-K line, the need for the high-resolution of HETGS to get information on the absorbers structures, and the value of NICER to study the strong soft excess.

Mrk 335

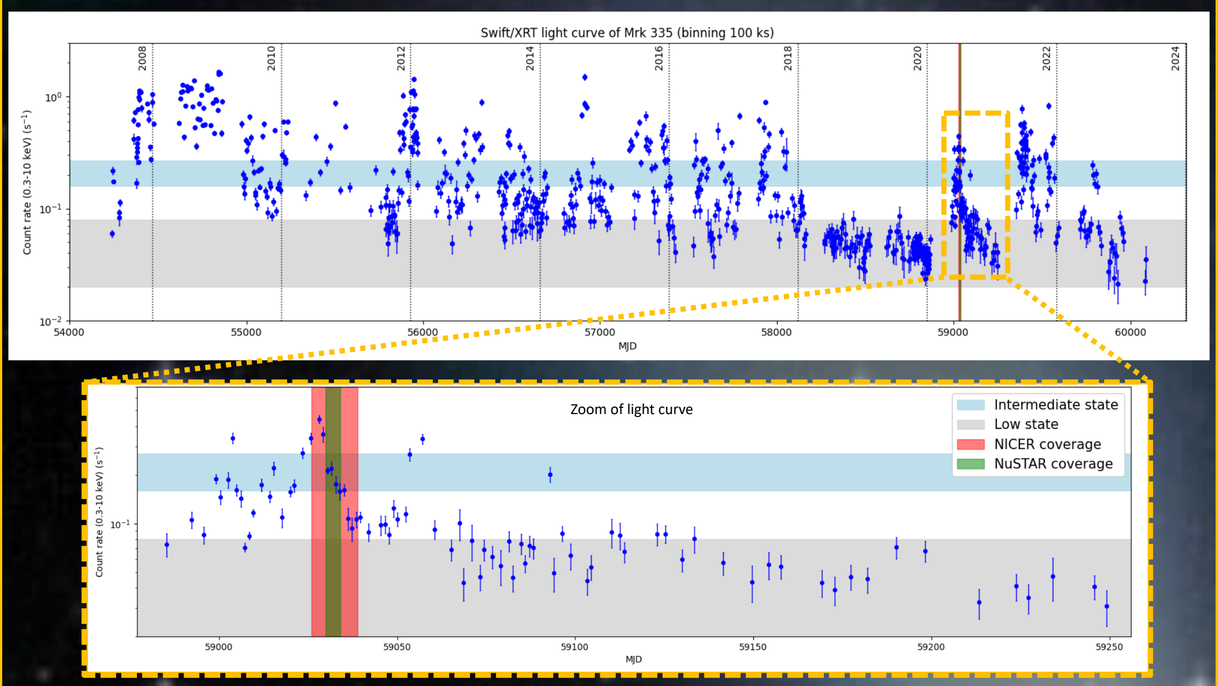

- Swift/XRT light curve ⇨ strong variability on both long and short time scales (Grupe et al. 2012)
- NLSy1 ⇨ typically strong soft excess
- Broad iron K line detected ⇨ signature of relativistic blurred reflection and/or partial covering absorption (Keek & Ballantyne 2016, Gallo et al. 2013, 2015)
- Several warm absorbers outflowing with a medium velocity, particularly visible in an intermediate state (Longinotti et al. 2013, 2019, Parker et al. 2019)
- Complex photoionized emission (Longinotti et al. 2008, Liu et al. 2021)
- Observations in June-July 2020 with Chandra/HETGS (240 ks), NuSTAR (100 ks), and NICER (10 ks) performed after the source recovered from its historically long low state
- $F_{2\text{-}10\ keV}$ = 4.05 – 5.27 x 10^{-12} erg cm^{-2} s^{-1} ⇨ intermediate flux state

Variability

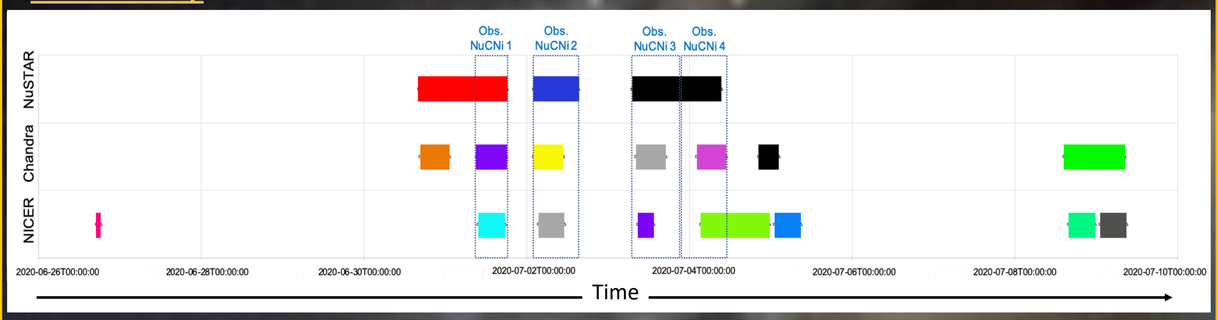

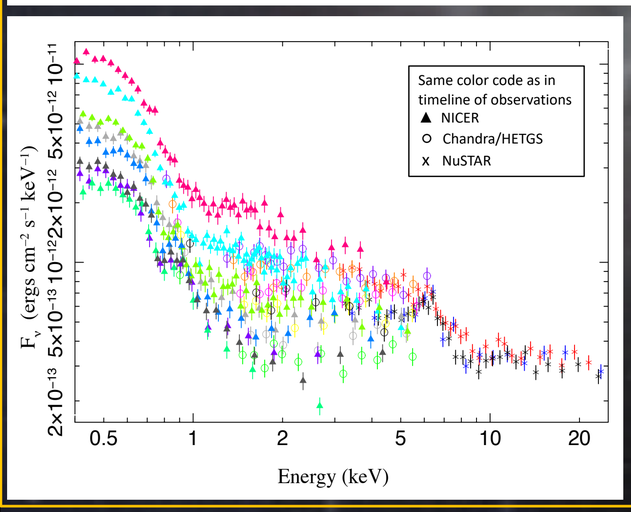

- Timeline of observations with the different satellites ⇨ division into 4 groups of simultaneous observations (NuCNi 1, 2, 3, and 4)
- Spectra of each individual observation shown in the timeline
- Rapid variability in flux and spectral shape ⇨ due to changes in the structure of the hot corona (Gallo et al. 2018, Wilkins et al. 2015, Kara et al. 2013), and to varying absorption (Longinotti et al. 2013, Komossa et al. 2020, Liu et al. 2021)

Spectral fitting

- Fit of the 4 groups of simultaneous observations NuCNi 1, 2 ,3 and 4
- Data binned to use χ^2 statistics
- Fit and MCMC performed with ISIS
- Cross-calibration factor used to fit the data from the different satellites
- Swift/BAT spectrum from the 105-months catalog, for better modeling the continuum

- Fit at high energy (>3 keV) with a cut-off powerlaw and a *XILLVER* component to model the distant reflection (Garcia et al. 2013)
- Contour plot of photon index vs reflection factor R ⇨ variable continuum
- Broad iron line detected in all groups of observations (≥90% CI, E∼5.5 keV, σ∼0.7keV, EW= 370-520 eV)

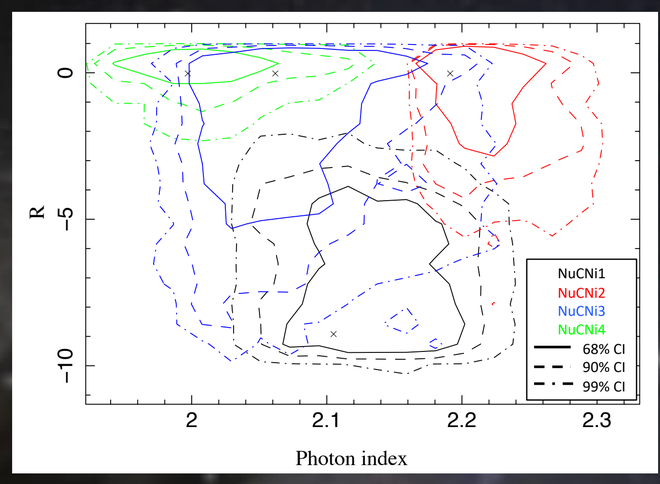

- After fitting the hard part, addition of data at lower energy and broadband modeling
- Strong soft excess modeled phenomenologically with a black body ⇨ stable

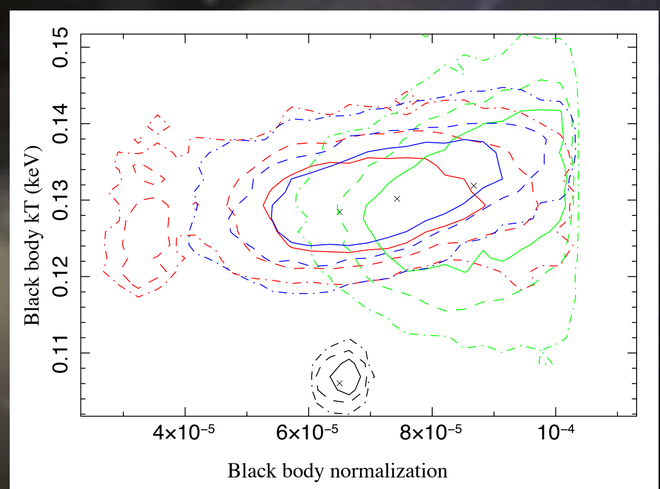

- Warm absorbers (WA) modeled with *zxipcf*
- First WA significantly detected in all observations (N_H = 2-3 x 10^{22} cm^{-2}, log(ξ) = 0.7-2.3, covering factor= 0.75-0.9, v_{out} = 3000-6000 km s^{-1}) ⇨ consistent with the denser component found by Longinotti et al. 2013
- Rapid variation of the absorbing material, in particular its ionization state

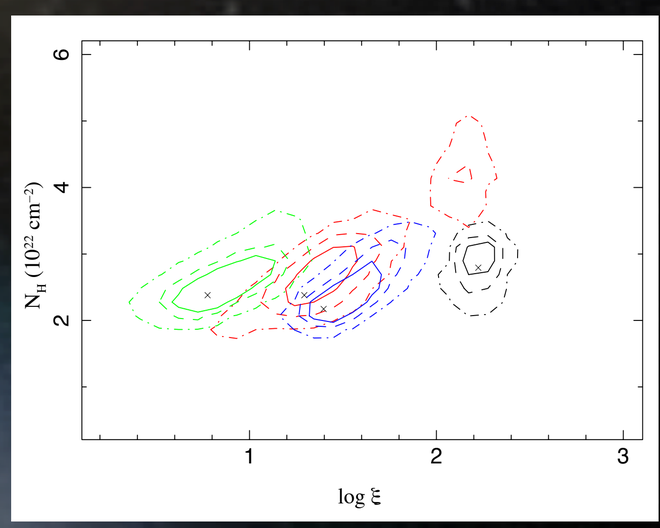

- Second WA marginally detected, poorly constrained (N_H=1.5-2.7 x 10^{21} cm^{-2}, log(ξ) ∼ 3, covering factor ∼ 1, v_{out} = 6000-7000 km s^{-1}) ⇨ may be consistent with the less dense component found by Longinotti et al. 2013
- No detection of the third WA found by Longinotti et al. 2013 ⇨ may still be present but de-ionized so featureless, or out of the line-of-sight due to transverse motion (Longinotti et al. 2013, Liu et al. 2021)

Ongoing analysis and next steps

- Use photoionization code *XSTAR* (Kallman et al. 2001) to model warm absorbers and photoionized emission, taking advantage of the high spectral resolution of Chandra/HETGS
- Test reflection (using *RELXILL*, Garcia & Dauser et al. 2014) and absorption scenari to explain the broadened iron K line and high energy spectrum (Keek & Ballantyne 2016, Gallo et al. 2013, 2015, Parker et al. 2019)
- Model the strong soft excess with a physical model (blurred reflection and/or warm Comptonization) to understand its nature (Keek & Ballantyne 2016, Petrucci et al. 2017, Boissay et al. 2016)

References Boissay R. et al., 2016, A&A, 588, 70 ❖ Gallo L. et al., 2013, MNRAS, 428, 1191 ❖ Gallo L. et al., 2015, MNRAS, 446, 633 ❖ Gallo L. et al., 2018, MNRAS, 478, 2557 ❖ Garcia J. et al., 2013, ApJ, 768, 146 ❖ Garcia J. & Dauser T. et al., 2014, ApJ, 782, 76 ❖ Grupe D. et al., 2012, The Astrophysical Journal Supplement Series, 199 ❖ Kallman T. et al. 2001, ApJS, 133, 221❖ Kara E. et al., 2013, MNRAS, 434, 1129 ❖ Keek L. & Ballantyne D., 2016, MNRAS, 456, 2722 ❖ Komossa S. et al., 2020, A&A, 643, L7 ❖ Liu H. et al., 2021, MNRAS, 506, 5190 ❖ Longinotti A. et al., 2008, A&A, 484, 311 ❖ Longinotti A. et al., 2013, ApJ, 766, 104 ❖ Longinotti A. et al., 2019, ApJ, 875, 150 ❖ Parker et al., 2019, MNRAS, 490, 683 ❖ Petrucci P.O. et al., 2017, A&A, 611, 59 ❖ Wilkins D. et al., 2015, MNRAS, 449, 129